Natural Resources for Human Health
eISSN: 2583-1194

Original Research

Received 10 May 2026
Revised 15 June 2026
Accepted 28 June 2026

Natural Resources for Human Health 2026, Vol. 6 (11s): 866–881

KEYWORDS:
Maternal exposure, Sulforaphane, Risperidone, St8sia2 and St8sia4 genes, Gene expression, Rat brain development, Histological analysis, PAS staining

The Effect of Risperidone on the Expression of the St8sia2 and St8sia4 Genes and Its Effect on the Glycocalyx Layer in the Brain Tissues of Embryos and Newborn Albino Rats

[1]Shelan Qader Sadeq, [2]Zubaida Adnan Kudair

[1]Tikrit University / College of Education for Women / Department of Biology
[2]Tikrit University / College of Education for Pure Sciences / Department of Life Sciences
E-mail: shmscbio@tu.edu.iq, zubaida.biology@tu.edu.iq

ABSTRACT: The present study investigated the effects of maternal exposure to sulforaphane (SFN) and risperidone (RIS) during pregnancy and the early postnatal period on the expression of the sialyltransferase genes St8sia2 and St8sia4 and the histological characteristics of developing rat brain tissue at embryonic day 14 (E14), the day of birth (P0), and postnatal day 7 (P7).

Histological examination using PAS staining revealed positive staining in all experimental groups, particularly in the intercellular matrix, neuronal membranes, and vascular structures, consistent with the presence of glycoprotein-rich components in developing brain tissue. At E14, the Saline group exhibited an organized cellular architecture with developing neurons and precursor cells, whereas the SFN group showed a more intense PAS reaction. The RIS group also demonstrated a positive PAS reaction with staining of the developing interstitial matrix and migrating neuronal cells. RT-qPCR results showed differences in the expression levels of the **St8sia2** and **St8sia4** genes among the experimental groups across the developmental stages. For **St8sia2**, no significant differences were observed between the Saline and SFN groups at any stage, whereas significant differences were detected between the RIS and SFN groups at **E14 (P = 0.0488)**, between the Saline and RIS groups at **P0 (P = 0.0327)**, and between the RIS and SFN groups (**P = 0.0015**). At **P7**, significant differences were observed between the Saline and RIS groups (**P = 0.0012**) and between the RIS and SFN groups (**P = 0.0001**). For **St8sia4**, no significant differences were observed among the experimental groups at **E14** or **P0**, whereas significant differences were detected at **P7** between the Saline and RIS groups (**P = 0.0139**) and between the RIS and SFN groups (**P = 0.0004**).

Conclusion: Maternal exposure to risperidone was associated with a significant reduction in *St8sia2* gene expression at P0 and P7 and in *St8sia4* expression at P7, compared with the Saline and/or SFN groups. In contrast, sulforaphane did not produce significant changes in the expression of either gene compared with the control group. PAS staining confirmed the presence of glycoprotein-rich components in developing brain tissue across all groups, with differences in staining intensity.

INTRODUCTION

The brain is a highly complex organ comprising millions of neurons that control and regulate the body; communication between individual neurons and their interaction with glial cells are essential for proper brain function. Every cell in the human body

whether endothelial, immune, muscle, blood, or neuronal exhibits a glycocalyx, which encodes a vast array of information critical to both health and disease and can be directly targeted in therapeutic contexts (Möckl, 2020). The glycocalyx is considered one of the most significant discoveries in histology and cell biology. The concept originated in the early 20th century when scientists observed a gelatinous coating covering cells; however, its chemical nature remained unclear until the mid-20th century(Richter and Sanderson, 2023; Foote *et al*., 2023). Sugars located at the outer termini of glycan chains often dictate the functional specificity of glycans. In mammals, glycoproteins and glycolipids frequently terminate with sialic acids—essential sugars typically found at the distal ends of glycans—enabling them to act as bridging molecules between cells, and between cells and the extracellular matrix (Schnaar *et al*., 2014; Yoo *et al*., 2015). The covalent addition of sialic acid to the termini of glycoproteins is known as sialylation; this critical biological modification plays a role in embryonic and neuronal development. During this process, sialic acid is added to the terminal ends of glycan chains on the cell membrane by a family of enzymes called sialyltransferases specifically St8sia2 and St8sia4. These enzymes polysialylate the glycans of a small subset of mammalian proteins; their most abundant substrate is the neural cell adhesion molecule (NCAM). They are responsible for adding polysialic acid (PSA/polysia) to various neuronal surface glycoproteins, thereby playing a central role in the formation of the neuronal glycocalyx (Zhu *et al*., 2024).

MATERIALS AND METHODS

Study Samples

This study utilized 18 healthy adult female albino laboratory rats, obtained from the laboratory animal breeding unit at the College of Veterinary Medicine, Tikrit University. The rats ranged in age from 11 to 12 weeks and in weight from (225 ± 10) grams. They were housed under standard laboratory conditions, including a temperature of 22–25°C and a 12-hour light/12-hour dark cycle, with continuous access to food and water.

Experimental Design

Mating was confirmed by pairing each female with an adult male and the day of vaginal plug observation was designated as Gestational Day 1. After confirmation of pregnancy, the females were randomly assigned into three main groups and housed in clean plastic cages. Different solutions were given to each group by oral gavage. This treatment was continued from Gestational Day 7 to Postnatal Day 7. The rats were weighed and general health monitored for any adverse effects of the drug.

Materials Administered to Rats

The first group (control) received an injection of physiological saline (NaCl) with a standard concentration of 0.9 %. Pregnant mothers were dosed orally at 1 ml daily starting 1 week after confirmation of pregnancy. Sulforaphane was used as the raw material, and it was obtained from Macklin (McIntyre and Johnson, 2025). Pregnant laboratory rats were given daily doses of 1 ml of the solution with 0.5 mg of raw sulforaphane per rat. Pregnant rats were administered raw risperidone (0.5 mg) (1 ml/rat).

Sample Collection Method

A total of 102 samples were collected across three distinct time points to investigate molecular and biochemical developmental changes in the three experimental groups. Animals were anesthetized using a chloroform solution. Fetal brains were collected on embryonic day 14 (E14): Pregnant dams (two per group) were dissected under sterile conditions; the uterus was opened, and the fetuses were carefully extracted (20 fetuses in the saline group, 21 in the sulforaphane group, and 19 in the risperidone group). Brains were then isolated using appropriate, precision dissection tools under conditions designed to preserve sample integrity. Neonatal rat brains were collected immediately after birth—postnatal day 0 (P0) (7–11) pups in the saline group, 9–11 in the sulforaphane group, and 9–11 in the risperidone group). Half of the pups from each group were separated from their mothers, anesthetized, and euthanized, while the remaining half were kept until one week after birth. Brains were then isolated from the neonates and preserved. Brains from young rats were collected one week after birth—postnatal day 7 (P7)—(comprising the second half of the pups, which had been reared and suckled by mothers that continued to receive the three experimental substances). These pups were separated from their mothers, anesthetized, and euthanized; their brains were then isolated using appropriate dissection tools under conditions ensuring sample preservation.

Sample Distribution According to Type of Analysis

Following extraction from the fetuses and newborns, the brains were divided into sections for the required tests, as follows: Brain tissue samples were preserved in Trizol solution and subsequently transferred to a deep freezer for storage at temperatures ranging from -20°C to -80°C; a total of 84 samples (derived from rat embryos and neonates) were collected for RNA extraction and molecular analysis specifically, the measurement of gene expression levels—using primers specific to the genes under investigation (ST8SIA2 and ST8SIA4). Additionally, whole brain samples (18 in total) were preserved in 10% formalin for histological examination using the Periodic Acid-Schiff (PAS) stain to assess the thickness and presence or absence of the glycocalyx on brain tissue cells.

Molecular Analysis

Specific primers were designed to detect and quantify the expression of the genes under study—specifically the sialyltransferase genes St8sia2 and St8sia4—using the NCBI Primer-BLAST tool; these primers were synthesized by Macrogen Inc. (Seoul, South Korea), as detailed in Table (1). Gene expression analysis was conducted on the three groups of rats to assess expression levels; this work was performed at the Central Laboratories Department at Tikrit University using a real-time PCR (RT-qPCR) system, with RNA extraction carried out using the TransZol Up Plus RNA Kit supplied by TRANS.

Table (1) Primer sequences used in the study, obtained using the Primer-BLAST tool available on the NCBI website.

Annealing	Size	Length	Sequence (5′-3′ direction)	Target Gene
Gene Expression Primers				
59	110	20	F AGCACAATGAACGTGTCCCA	St8sia2
59	110	20	R AGCAAGACTCCTGAGTTGCC	
59	110	20	F ATAGCCAGGACTGAGGAGCA	St8sia4
59	110	20	R GACCAGCCTTCCGAGTGAT	
Housekeeping Gene				
59	143	20	F GGAGAAACCTGCCAAGTATG	GAPDH
59	143	21	R TGATGGTATTCGAGAGAAGGG	

RNA was converted into complementary DNA (cDNA) using the activity of the reverse transcriptase enzyme. Following the additions, the samples were transferred to a thermocycler, and the reaction was initiated according to the program outlined in Table (2).

Table (2) RT-qPCR reaction program

Step	Time(min-sec)	Temp. °C	Cycle
Enzyme activation	60 sec	95	1
Denaturation	15 sec	95	40-45
Extension	30 sec	60	-
Melt Curve	5 sec	60-90	1

Gene Expression

To measure the level of gene expression, the following equations were used (Livak and Schmittgen, 2001): Analysis of relative gene expression data using real-time quantitative PCR and the $2^{(-\Delta\Delta Ct)}$ method.

Natural Resources for Human Health
eISSN: 2583-1194

Histological Examinations

Upon completion of the dosing period for the rat groups under study, the animals were anesthetized with chloroform and dissected. The target organs—specifically the brains of the fetuses and newborns—were excised, and histological sections were prepared according to the methods of Al-Hajj.(2010)

Statistical Analysis

Gene expression data for the ST8SIA2 and ST8SIA4 genes were analyzed using GraphPad Prism (Version 10) software. One-way ANOVA was employed to compare experimental groups at each time point individually, while two-way ANOVA was used to analyze differences between experimental groups across the three developmental stages. Tukey's multiple comparisons test was conducted to determine differences between groups. Results are presented as mean ± standard deviation (Mean ± SD), with a P-value < 0.05 considered statistically significant.

RESULT

Using the RT-qPCR technique and the GAPDH gene as a reference across all 84 samples from the three experimental groups (RIS, SFN, and Saline), the melting curves exhibited sharp definition and narrow peaks—indicating the production of homogeneous and pure PCR products—as illustrated in Figure (1).

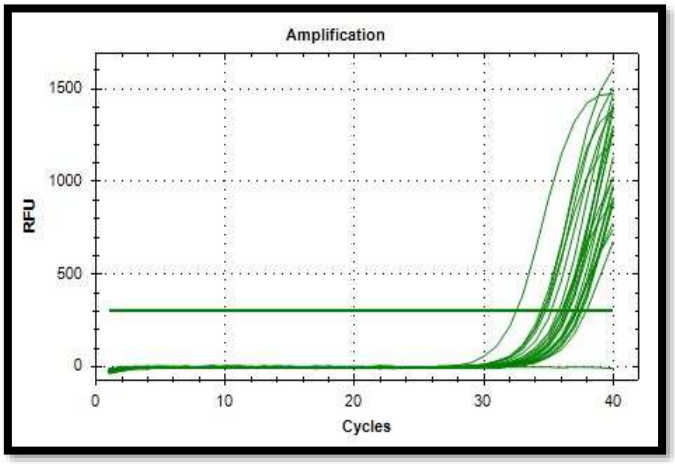

Figure (1) shows the RT-qPCR amplification curve for the study samples, with amplification beginning approximately between cycles 30 and 35.

The properties of double-stranded DNA (deoxyribonucleic acid) can be evaluated using melting curve analysis. This curve assesses the dissociation characteristics of DNA during heating; as the temperature rises, the double strands begin to separate, leading to an increase in absorbance (hyperchromicity). The temperature at which 50% of the DNA is denatured is known as the melting temperature, as illustrated in Figure (2).

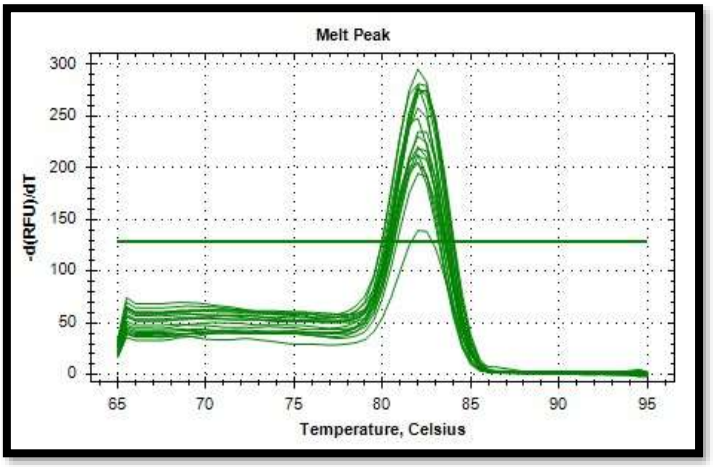

Figure (2) Melting peak curves of qPCR products for the study samples.

RT-qPCR analysis was performed on samples from the experimental groups across developmental stages using specific primers. At the embryonic stage (E14), the mean gene expression values (mean folding ± SD) were 0.94 ± 0.46 for the Saline group, 1.25 ± 1.03 for the SFN group, and 0.46 ± 0.32 for the RIS group Table (3). One-Way ANOVA results regarding St8sia2 gee expression levels across the three experimental groups at stage E14 revealed no statistically significant differences between the Saline and SFN groups (P = 0.5092) or between the Saline and RIS groups (P = 0.2103). However, the comparison between the RIS and SFN groups yielded a P-value of 0.0488, as illustrated in Figure (3). At the day of birth (P0), the mean value of gene expression for the Saline group was 1.06 ± 1.06, whereas the mean for the SFN group rose to 1.52 ± 1.10, while it decreased to 0.16 ± 0.23 in the RIS group. Statistical analysis revealed no significant difference between the Saline and SFN groups (P = 0.3340). Conversely, there were significant differences between the Saline and RIS groups (P = 0.0327) and between the RIS and SFN groups (P = 0.0015), Figure (4). At the one-week postnatal stage (P7), the mean gene expression value for the Saline group was 1.18 ± 0.69, whereas the mean for the SFN group rose to 1.57 ± 1.11 while it dropped to 0.06 ± 0.07 in the RIS group. Statistical analysis revealed no significant difference between the Saline and SFN groups (P = 0.3547). Conversely, there were clear significant differences between the Saline and RIS groups (P = 0.0012), as well as between the RIS and SFN groups (P = 0.0001), as illustrated in Figure (5)

Table (3) Mean gene expression of the St8sia2 gene in experimental groups at developmental stages.

Developmental stages	Treatment	Gene Expression (mean ± SD)
E14	Saline	0.94 ± 0.46
	SFN	1.25 ± 1.03
	RIS	0.46 ± 0.32
P0	Saline	1.06 ± 1.06
	SFN	1.52 ±1.10
	RIS	0.16 ± 0.23
P7	Saline	1.18 ± 0.69
	SFN	1.57 ± 1.11
	RIS	0.06 ± 0.07

Natural Resources for Human Health
eISSN: 2583-1194

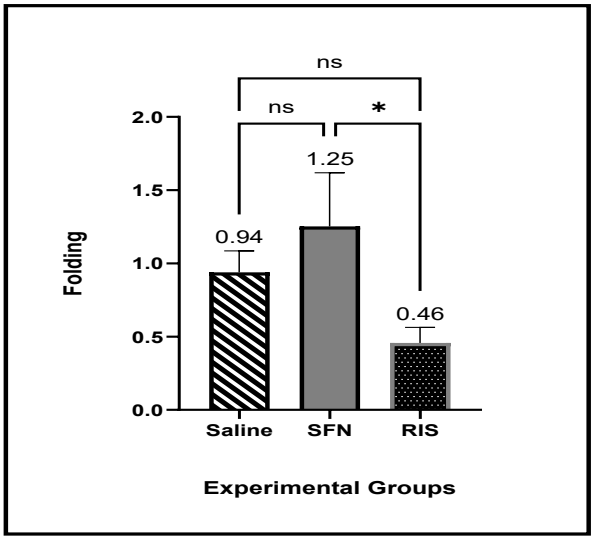

Figure (3) Gene expression levels of the St8sia2 gene in experimental groups at stage E14.

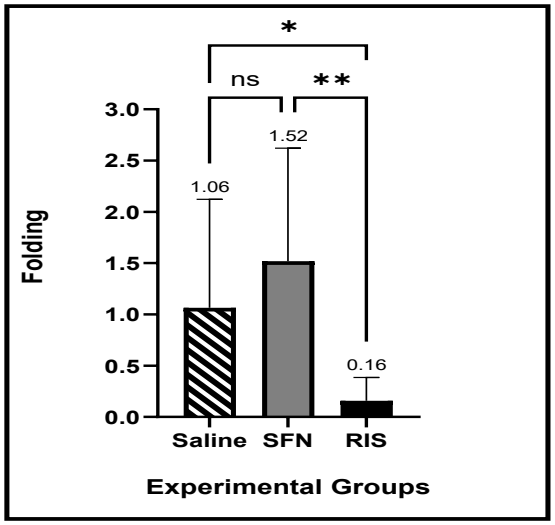

Figure (4) Gene expression levels of the St8sia2 gene for the experimental groups at the P0 stage.

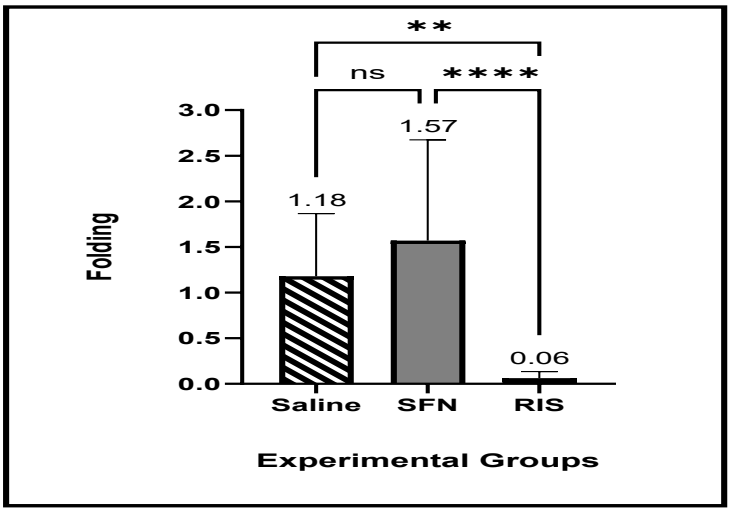

Figure (5) Gene expression levels of the St8sia2 gene for the experimental groups at the P7 stage.

The results revealed a gradual upward trend in gene expression levels as developmental stages progressed, particularly in the control and sulforaphane groups; conversely, the risperidone group exhibited a clear downward trend in gene expression from the embryonic stage (E14) through the stage immediately following birth (P0) to the one-week postnatal stage (P7). Comparisons showed no significant differences among the three stages, with all p-values exceeding 0.05 (as shown in Table (4) and Figure (6).

Table (4) Results of multiple comparisons for (St8sia2 gene expression across developmental stages.

Treatment	Comparisons	Adjusted P Value
Saline	E14 vs P0	ns 0.9042
	E14 vs P7	ns 0.4264
	P0 vs P7	ns 0.1413
SFN	E14 vs P0	ns 0.4226
	E14 vs P7	ns 0.4790
	P0 vs P7	ns 0.1590
RIS	E14 vs P0	ns 0.5574
	E14 vs P7	ns 0.3867
	P0 vs P7	ns 0.9627

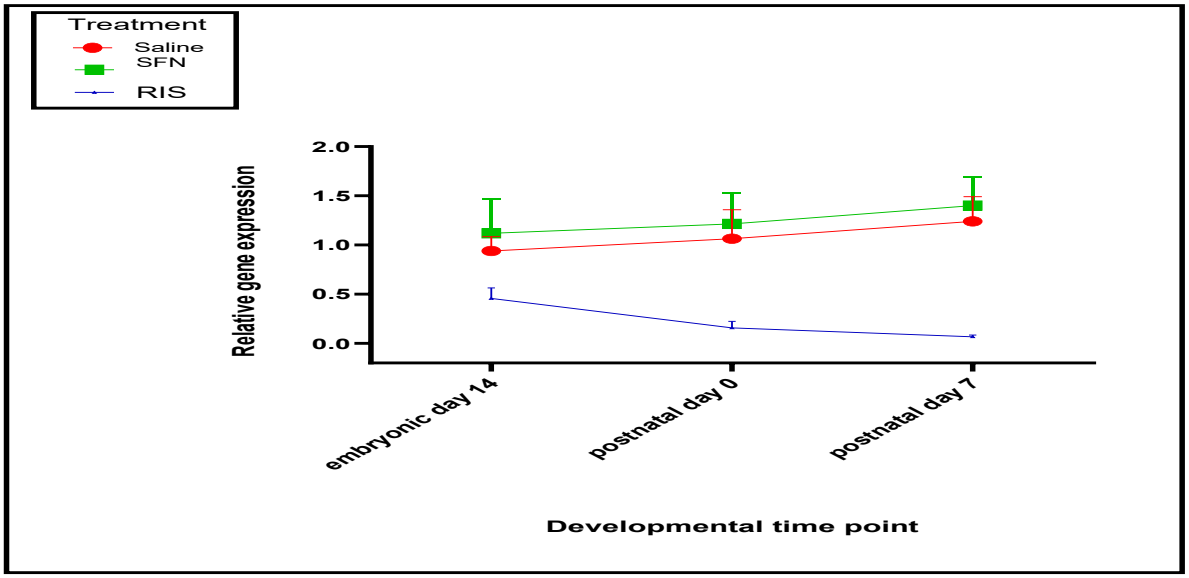

Figure (6) Changes in relative gene expression levels of the St8sia2 gene during developmental stages

RT-qPCR analysis was performed on samples from the three groups across three time points using primers specific to the St8sia4 gene. At the embryonic stage (E14), the mean gene expression values (mean folding ± SD) were 0.87 ±1.28 for the Saline group, 1.15 ± 0.81 for the SFN group, and 0.59 ± 0.31 for the RIS group, as shown in Table (5). The results comparing St8sia4 expression levels among the three experimental groups at stage E14 revealed no statistically significant differences ($P = 0.7798$) between the Saline and SFN groups, ($P = 0.7498$) between the Saline and RIS groups, and ($P = 0.4476$) between the RIS and SFN groups, as illustrated in Figure (7).

At the day of birth (P0), the mean value of gene expression for the Saline group was 0.81 ± 0.75; (1.05 ± 0.74) in the SFN group, (0.53 ± 0.28) in the RIS group, as shown in Table (5). Statistical analysis revealed no significant differences between the

Saline and SFN groups (P = 0.5904), no significant differences between the Saline and RIS groups (P = 0.4968), and no significant differences between the RIS and SFN groups (P = 0.1259), as illustrated in Figure (8).

At the one-week postnatal stage (P7), the mean gene expression value for the Saline group was 1.04 ± 0.75; the mean increased to 1.34 ± 0.98 in the SFN group, 0.24 ± 0.18 in the RIS group Table (5). Statistical analysis revealed no significant difference between the Saline and SFN groups (P = 0.4682). Conversely, significant differences were observed between the Saline and RIS groups (P = 0.0139) and between the RIS and SFN groups (P = 0.0004), Figure (9).

Table (5) Mean gene expression of the St8sia4 gene in experimental groups at developmental stages.

Developmental stages	Treatment	Gene Expression (mean ± SD)
E14	Saline	0.87 ± 1.28
	SFN	1.15 ± 0.81
	RIS	0.59 ± 0.31
P0	Saline	0.81 ± 0.75
	SFN	1.05 ± 0.74
	RIS	0.53 ± 0.28
P7	Saline	1.04 ± 0.75
	SFN	1.34 ± 0.98
	RIS	0.24 ± 0.18

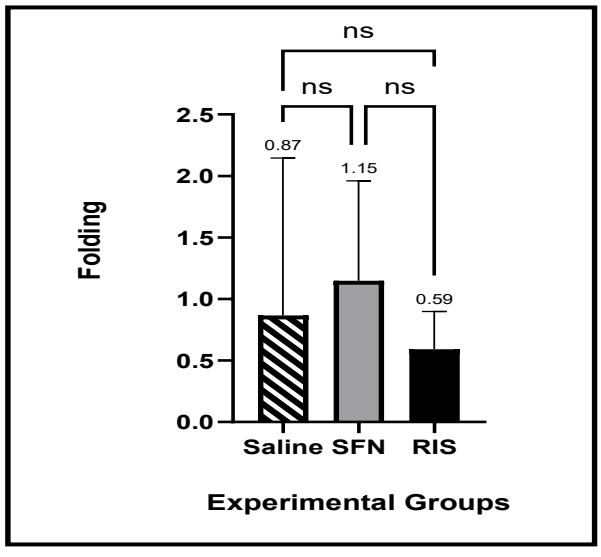

Figure (7) Gene expression levels of the St8sia4 gene for the experimental groups at stage E14.

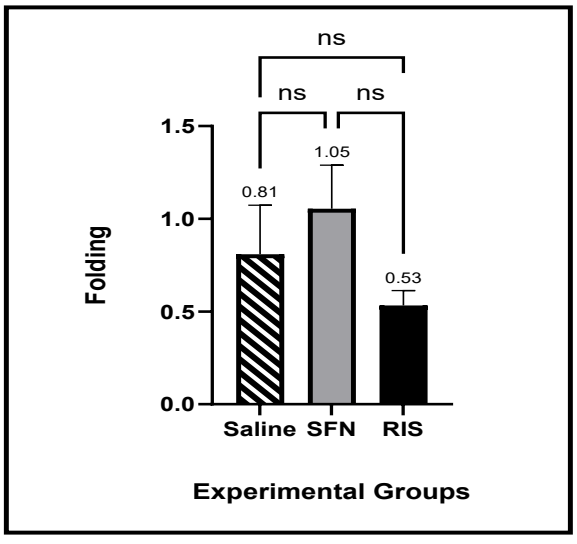

Figure (8) Gene expression levels of the St8sia4 gene in experimental groups at stage P0.

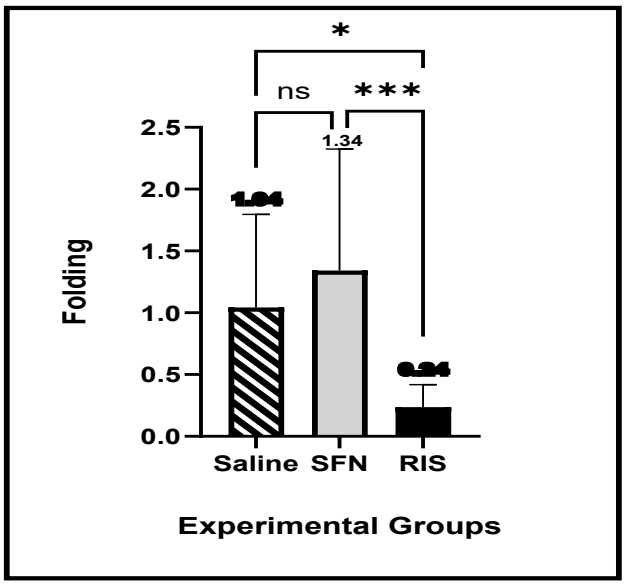

Figure (9) Gene expression levels of the St8sia4 gene in experimental groups at the P7 stage.

Two-way ANOVA results indicated stable gene expression levels across developmental stages, particularly in the control and sulforaphane groups; conversely, the risperidone group exhibited a clear downward trend in gene expression levels from the day-of-birth stage (P0) through the one-week post-natal stage (P7). Comparisons between developmental stages within each group using Tukey's multiple comparisons test revealed no significant differences among the three stages, with all p-values exceeding 0.05 ,as shown in Table (6). These results demonstrate that temporal changes in St8sia4 gene expression levels within the study groups did not show significant variation (as illustrated in Figure (10).

Table (6) Results of multiple comparisons for St8sia4 gene expression across developmental stages.

Treatment	Comparisons	Adjusted P Value
Saline	E14 vs P0	ns 0.1713
	E14 vs P7	ns 0.1196
	P0 vs P7	ns 0.5315
SFN	E14 vs P0	ns 0.9686
	E14 vs P7	ns 0.4154
	P0 vs P7	ns 0.4610
RIS	E14 vs P0	ns 0.9831
	E14 vs P7	ns 0.5119
	P0 vs P7	ns 0.5751

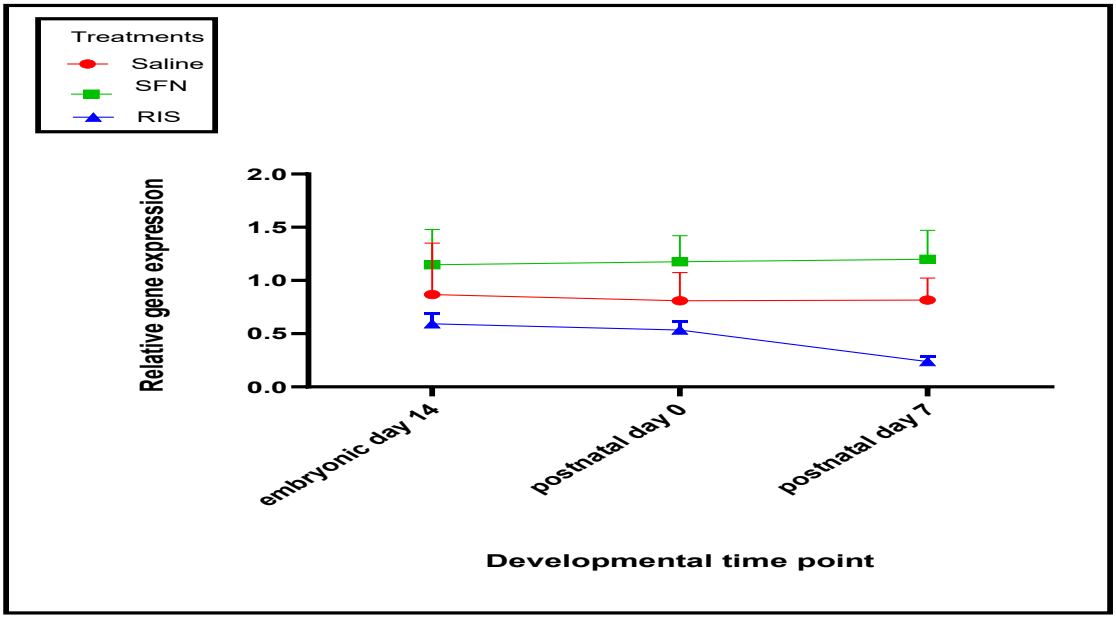

Figure (10) Changes in relative gene expression levels of the St8sia4 gene during developmental stages.

Microscopic examination of brain tissue sections from rat foetuses and newborns (18 samples in total, at different developmental stages: E14, P0, P7 and three experimental groups: Saline, SFN, RIS) revealed a uniform positive reaction to the Periodic Acid-Schiff (PAS) stain. Purple staining of the intercellular matrix, neuronal membranes and vascular cells is indicative of normal levels of sialic acid containing glycoproteins during physiological development. E14. Microscopic image of the foetal brain tissue section: First, the control group (Saline) exhibits a uniform and intact cellular structure. The tissue is characterized by a high density of neurons and developing precursor cells (neuroblasts and glioblasts) with distinct round and oval nuclei; these cells are arranged in an organized pattern indicating cellular migration pathways and the onset of fiber bundle formation. The tissue also shows a positive PAS reaction in blood vessels and developing capillaries due to the glycoprotein-rich nature of their basement membranes—along with mild to moderate positivity in the surrounding interstitial matrix (as shown in Figure 11).

In the Sulforaphane (SFN) group, the fetal brain tissue section displays a very distinct positive response to the PAS stain. The stain appears intensely, reflecting the abnormal deposition of glycoproteins and fetal interstitial matrix components, thereby illustrating the biochemical distribution within the developing nervous tissue (as shown in Figure 12). Thirdly: The histological section of the foetal brain in the Risperidone (RIS) group is characterised by a specific and normal positive PAS response, with an intense staining due to the presence of a large number of glycoproteins and embryonic interstitial matrix, which are a reflection of the biochemical distribution of the components of the developing nervous tissue, while the columns of migrating neurones and neuroblasts are characterised by the presence of a moderate pink cytoplasmic staining, as shown in Figure (13).

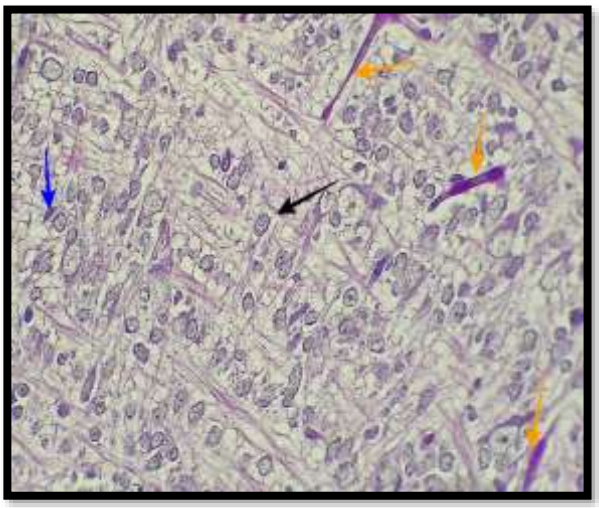

Figure (11): Brain tissue section of a 14-day-old rat fetus from the control group (saline), showing the differential reactivity of developing nervous tissue components. Orange arrows indicate developing blood vessels and capillaries exhibiting intense positive staining; the blue arrow points to neuroblasts; and the black arrow indicates densely packed developing glioblasts, which show moderate positive reactivity to PAS staining (400x).

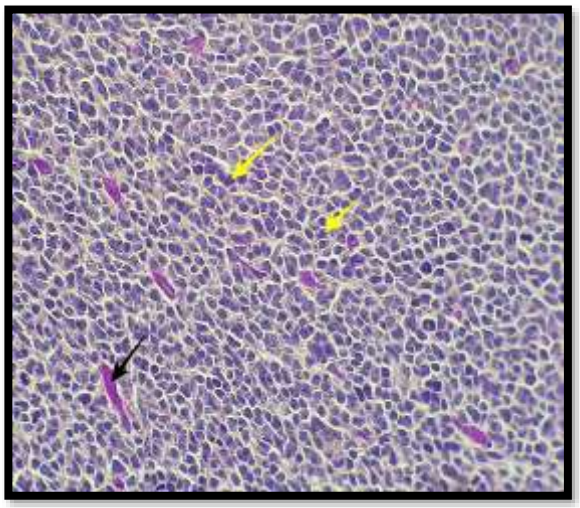

Figure (12): Brain tissue section of a 14-day-old rat fetus from the SFN group, showing the differential reactivity of developing neural tissue components. Yellow arrows indicate densely packed, PAS-positive neuroblasts, while the black arrow points to developing capillaries that are intensely stained with PAS due to glycoprotein deposition in the basement membrane (400x).

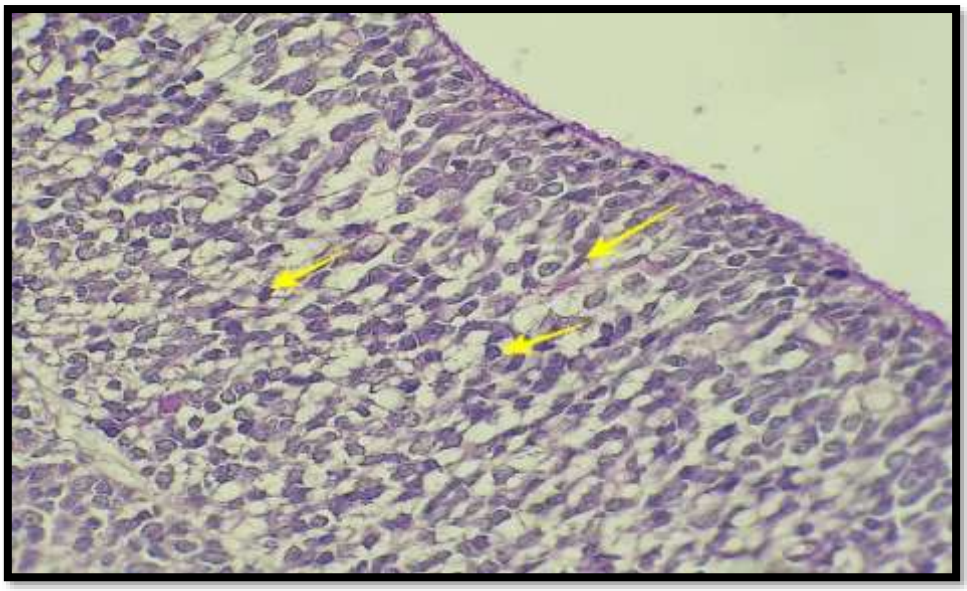

Figure (13): Brain tissue section of a 14-day-old rat fetus from the RIS group, showing the differential reactivity of the developing nervous tissue components; yellow arrows indicate densely packed, PAS-positive neuroblasts (400x).

For the results obtained at birth day (P0), the control group (saline treated) showed distinct patterns of cellular reactivity. Areas of very high cellular density were identified composed of tightly packed immature neurones and glioblasts with dark chromatin dense nuclei. Conversely, the developing blood vessels and capillaries were strongly PAS positive, with the endothelial walls and basement membranes staining a distinct purple, reflecting the high content of carbohydrates and glycoproteins associated with active angiogenesis at this early stage of development. Also seen were developing astrocytes with pale, spherical, vesicular

nuclei and a faintly reactive, spider-web or spongy cytoplasmic network within the neuropil. Between these were cells with elongated or spindle-shaped cytoplasmic processes known as pyramidal cells which had weak to moderate staining reactivity and this indicates the early stages of structural formation and development of neural tissue components during the early developmental period as shown in Figure (14). Secondly, in the Sulforaphane (SFN) group, microscopic examination of the tissue reveals a distinct contrast in PAS staining intensity intense, concentrated staining is observed in the basement membranes and blood vessel walls owing to their high glycoprotein content—along with a strong reaction in neuronal nuclei, as shown in Figure (15).

Thirdly, regarding the Risperidone (RIS) group, microscopic examination of the PAS-stained tissue section reveals a clear variation in color reaction intensity; the highest staining intensity is concentrated in the walls of blood vessels and developing capillaries, reflecting the glycoprotein-rich nature of their basement membranes. Meanwhile, the staining intensity transitions to moderate and faint levels within the tissue matrix and glial cells, indicating a moderate distribution of cytoplasmic carbohydrates throughout the nervous tissue, as shown in Figure(16).

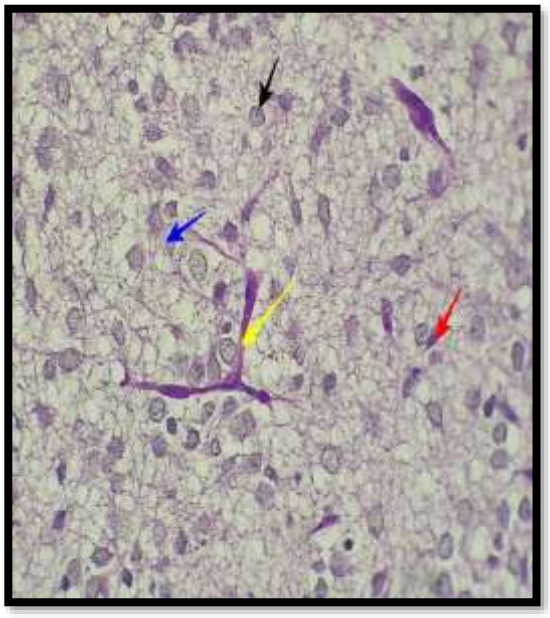

Figure (14): Brain tissue section of a fetus from the saline group, one day after birth, showing the differential reactivity of the developing nervous tissue components. Black arrows indicate the closely packed, dark nuclei of neurons and glial cells, which are negative or weakly reactive to the PAS stain; yellow arrows point to the basement membranes of developing blood vessels, which exhibit a strong positive reaction to the stain; blue arrows indicate neuronal processes; and red arrows point to a pyramidal neuron (400x).

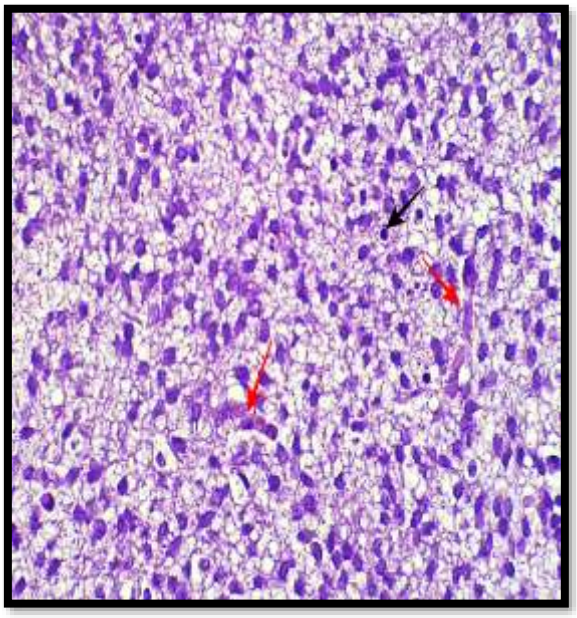

Figure (15): Brain tissue section of a neonatal rat from the SFN group, showing the differential reactivity of developing neural tissue components. The black arrow indicates PAS-positive glial cell nuclei, while the red arrows point to the basement membranes of developing blood vessels, which exhibit a strong positive reaction to the stain (400x)

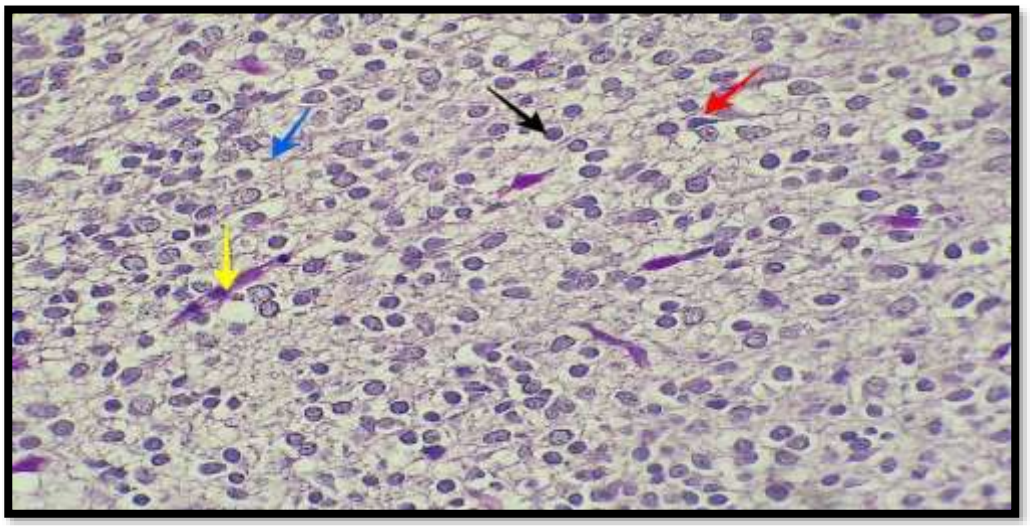

Figure (16): Brain tissue section of a young rat from the RIS group, one day after birth, showing the differential reactivity of developing nervous tissue components. The black arrow indicates glial cell nuclei that are PAS-positive, while the yellow arrow points to the basement membrane of developing blood vessels, which exhibits a strong positive reaction to the stain. The blue arrow indicates neuronal processes, and the red arrow points to a pyramidal-shaped neuron (400x)..

Microscopic examination of histological sections from rat brains at postnatal day 7 (P7): First, examination of PAS-stained sections from the control group revealed distinct variations in cellular reactivity. Regions of very high cellular density were observed, consisting of tightly packed, mature, spindle-shaped pyramidal neurons with dark, chromatin-dense nuclei. In contrast, developing blood vessels and capillaries exhibited strong PAS positivity; their endothelial walls and basement membranes stained distinctly purple, reflecting a high content of carbohydrates and glycoproteins. Glial cells were also observed, characterized by pale, spherical, vesicular nuclei set against a faintly reactive, spider-web-like or spongy cytoplasmic network (neuropil); these were interspersed with cells featuring extended cytoplasmic processes that showed moderate staining reactivity, as illustrated in Figure (17). Second: In the Sulforaphane (SFN) group, a histological section of the rat brain examined one week after birth exhibits a distinct positive response to PAS staining; the stain appears intense due to glycoprotein deposition. Capillaries within the tissue also show a positive reaction, as their endothelial lining cells are rich in glycoproteins (see Figure 18).

Third: In the Risperidone (RIS) group, microscopic examination of the PAS-stained histological section reveals the highest staining intensity in the walls of blood vessels and developing capillaries, owing to the glycoprotein-rich nature of their basement membranes. Additionally, pyramidal neurons exhibit a positive reaction, whereas staining intensity ranges from moderate to faint in the tissue matrix and glial cells, indicating a moderate cytoplasmic carbohydrate distribution within the nervous tissue (see Figure 19).

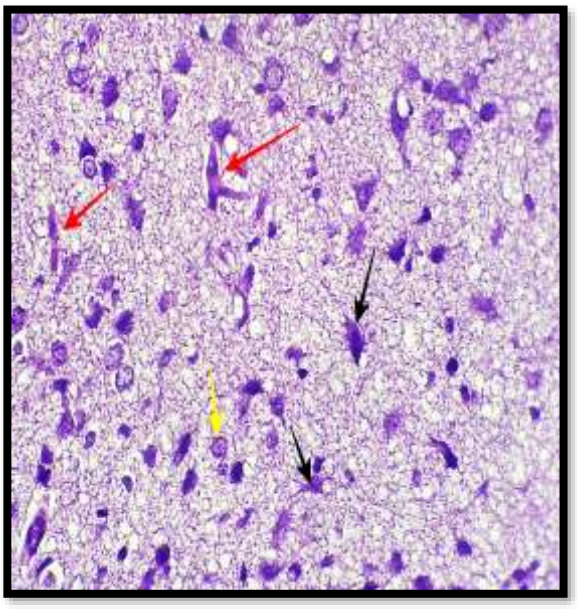

Figure (17): A section of brain tissue from a rat pup in the control group (saline) one week after birth, showing the differential reactivity of neural tissue components. The black arrow points to the nuclei of pyramidal neurons that are positive for the PAS stain, and the yellow arrow points to glial cell nuclei, while the red arrows indicate the basement membranes of blood vessels, which exhibit a strong positive reaction to the stain (400x)

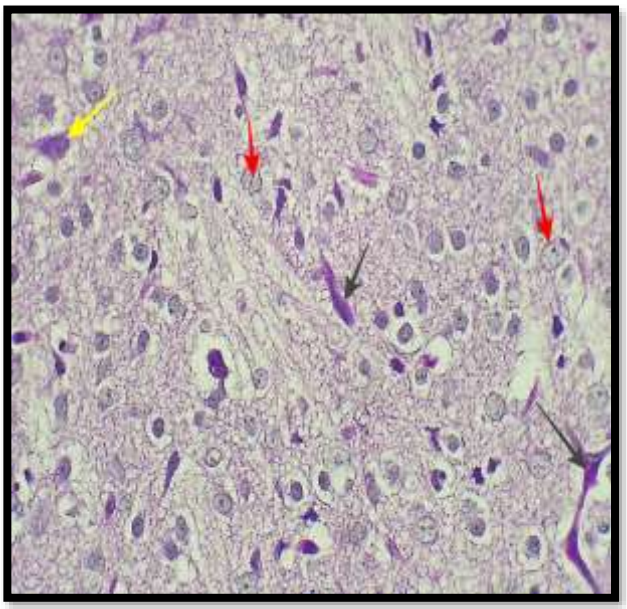

Figure (18): A section of brain tissue from the SFN group (neonates, one week after birth) showing the differential staining reaction of neural tissue components. The yellow arrow indicates pyramidal neurons that are positive for the PAS stain; the black arrow points to developing capillaries; and the red arrow indicates glial cell nuclei showing a moderate staining response (400x)

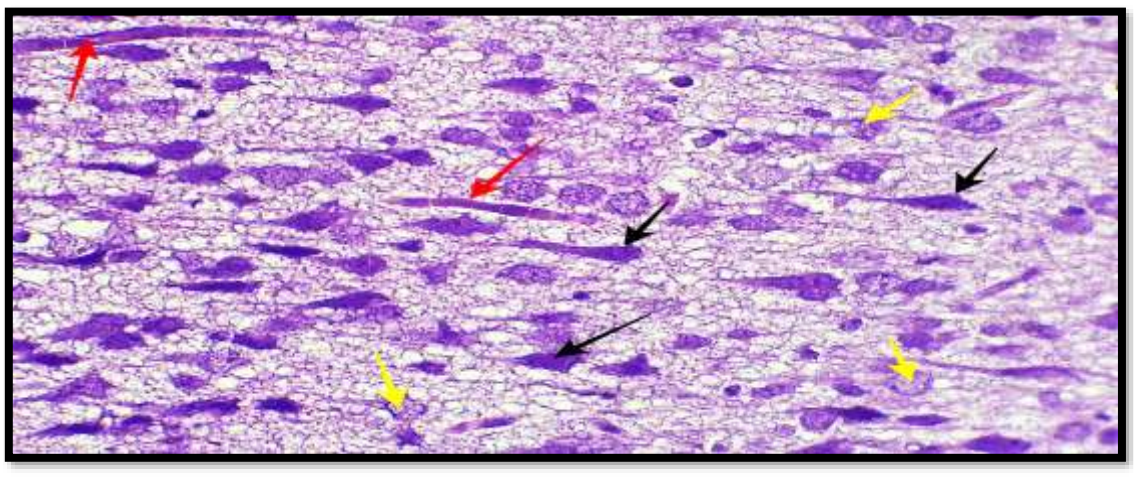

Figure (19): A section of brain tissue from a rat pup in the RIS group, one week after birth, showing the differential staining reaction of neural tissue components. The black arrow points to the nuclei of pyramidal neurons and their processes, which are positive for the PAS stain; the yellow arrow indicates the lightly stained nuclei of glial cells; and the red arrows point to the basement membranes of blood vessels, which exhibit a strong positive reaction to the stain (400x).

Natural Resources for Human Health
eISSN: 2583-1194

DISCUSSION

The present study showed a developmental-stage-dependent pattern of the St8sia2 and St8sia4 gene expression after maternal exposure to sulforaphane (SFN) and risperidone (RIS). At E14, RIS and SFN differed significantly. This pattern suggests that the effect of RIS on St8sia2 expression may already be detectable during embryonic development. (Schuster *et al.* ,2020) demonstrated loss of St8sia2 in mice changed the directional persistence and branching behaviour of migrating interneurons and affected the distribution of parvalbumin-positive interneurons in the developing cortex. Expression at P0 decreased in the Saline group and RIS group, while the SFN group had a slightly higher mean expression. This finding suggests that the downregulation of St8sia2 expression caused by RIS exposure was more pronounced around the time of birth. This timing is relevant because ST8SIA2 is especially relevant during embryonic and perinatal development. (Curto *et al.* ,2019) reported that ST8SIA2 expression is prominent in embryonic and perinatal stages and declines afterward, whereas ST8SIA4 has a relatively different temporal profile. (Kobayashi *et al.* ,2017) showed that although both enzymes are involved in polySia synthesis, ST8SIA2 and ST8SIA4 produce polysialic acid chains with different characteristics. Moreover, (Szewczyk *et al.* 2017) showed that ST8SIA2 deficiency in mice was associated with impaired oligodendrocyte differentiation, reduced myelin content, thinner myelin sheaths, and axonal abnormalities. (Werneburg *et al.* ,2017) demonstrated that the two polysialyltransferases have opposing effects during oligodendrocyte differentiation, with ST8SIA2 supporting early oligodendrocyte differentiation, whereas ST8SIA4 becomes more prominent during later stages. (Küçükerden *et al.* ,2022) showed that selective deletion of St8sia2 in different brain regions resulted in abnormalities in particular neural pathways, including the mammillary body and mammillothalamic tract, and was linked to altered behavioural phenotypes. (Curto *et al.* ,2019) showed that ST8SIA4 depletion led to reduced dendritic complexity, while depletion of either ST8SIA2 or ST8SIA4 affected the density of parvalbumin-positive perisomatic synaptic structures. These results suggest that the two enzymes can contribute both overlapping and distinct contributions to neuronal connectivity. The current findings are also consistent with previous empirical evidence on prenatal RIS exposure. (Singh *et al.* 2016) reported developmental neurotoxicity induced by prenatal RIS exposure in rats including decrease in fetal brain size and weight, changes in neocortical architecture and apoptotic neurodegeneration. In a related study, (Singh and Singh ,2017) reported that in utero RIS exposure produced structural abnormalities in the developing hippocampus and striatum and was associated with cognitive impairment in offspring. (Han *et al.* 2017) reported that low concentrations of SFN promoted neural stem-cell proliferation and neuronal differentiation and were associated with activation of Wnt signaling. Therefore, the relatively higher expression values observed in the SFN group may be compatible with a broader neurobiological effect of SFN, but the present data do not establish a direct effect of SFN on *St8sia2* or *St8sia4* transcription.

Histological results using PAS staining showed that the control group maintained normal methylation status, physiological gene expression, balanced sialic acid metabolism, and proper regulation of the glycocalyx layer, resulting in normal tissue structure throughout all stages of development .Numerous previous studies corroborate the histological improvements observed in the sulforaphane group, highlighting the neuroprotective properties of this natural isothiocyanate; (Campisi *et al.* ,2025). Another study demonstrated that sulforaphane protects the nervous system against the toxic effects of environmental pollutants and combats tissue and cellular damage caused by advanced glycation end-products (facilitating detoxification)(Fahey *et al.*, 2025). A study reported that sulforaphane protects nervous tissue—and consequently neurons—from oxidative stress-induced apoptosis by upregulating intracellular antioxidant enzymes and reducing reactive oxygen species; histological analysis following sulforaphane treatment revealed improved neuronal survival and reduced degeneration (Tarozzi *et al.*, 2013). Biological, maternal Risperidone exposure depresses sialyltransferase activity and polysialic acid synthesis in developing fetal and neonatal brains, disrupting neuronal glycocalyx integrity and impairing cellular migration and tissue architecture. These findings align with previous studies showing that in utero Risperidone exposure induces structural abnormalities in the fetal and offspring hippocampus, streatum, and neocortex, leading to neurodegeneration (Singh *et al.* , 2016 ; Singh and Singh, 2017)

REFERENCES

[1] Al-Hajj, Hamid Ahmed (2010). *Light Microscopic Preparations: Theory and Practice*. Dar Al-Masirah for Publishing, Distribution, and Printing. First Edition, Amman, Jordan, p. 238.

[2] Campisi, M. ; Cannella, L. ; Visioli, F. ; Pavanello, S. (2025a) Mechanistic insights and perspectives for healthy aging . Advances in Nutrition . 100521.

[3] Curto, Y., Alcaide, J., Röckle, I., Hildebrandt, H. and Nacher, J. (2019). Effects of the genetic depletion of polysialyltransferases on the structure and connectivity of interneurons in the adult prefrontal cortex. Frontiers in Neuroanatomy, 13, 6. DOI: 10.3389/fnana.2019.00006.

[4] Fahey, J. W. ; Liu, H. ; Batt, H. ; Panjwani, A. A. ; Tsuji, P. (2025) Sulforaphane and brain health: from pathways of action to effects on specific disorder . Nutrients. 17(8): 1353 .

[5] Foote, C. A. ; Soares, R. N. ; Ramires-Peres, F. I. ;Ghiarone, T. ; Aroor, A. ; Manrique-Acevedo, C. ; Padilla, J. ; Martinez-Lemus,L.A. (2023) Endothelial Glycocalyx . Compr Physiol. 12(14):3781-3811 .

[6] Han, Z., Xu, Q., Li, C. and Zhao, H. (2017). Effects of sulforaphane on neural stem cell proliferation and differentiation. Genesis, 55, e23022. DOI: 10.1002/dvg.23022.

[7] Kobayashi, T. *et al.* (2017). Different properties of polysialic acids synthesized by the polysialyltransferases ST8SIA2 and ST8SIA4. Glycobiology. DOI: 10.1093/glycob/cwx057.

[8] Küçükerden, M. *et al.* (2022). Compromised mammillary body connectivity and psychotic symptoms in mice with di- and mesencephalic ablation of ST8SIA2. Translational Psychiatry, 12, 51. DOI: 10.1038/s41398-022-01816-1.

[9] Livak, K. J. and Schmittgen, T. D. (2001) Analysis of relative gene expression data using real-time quantitative PCR and the 2-ΔΔCT method . Methods . 25(4):402-408 .

[10] Mcintyre, C. and Johnston, B. (2025) Sulforaphane – Uses, Side Effect, and More. WebMD .

[11] Möckl, L. (2020) The Emerging Role of the Mammalian Glycocalyx in Functional Membrane Organization and ImmuneSystem Regulation . *Frontiers in cell developmental biology*. 8:253 .

[12] Richter, J. R. and Sanderson, R. D. (2023) The Glycocalyx: pathobiology and repair. Matrix biology plus. 17: 100128.

[13] Schnaar, R. L. ; Gerardy-Schahn, R. ; Hildebrandt, H. (2014) Sialic acids in the brain: gangliosides and polysialic acid in nervous system development, stability, disease, and regeneration . Physiological reviews. 94(2): 461-518 .

[14] Schuster, U.E., Rossdam, C., Röckle, I., Schiff, M. and Hildebrandt, H. (2020). Cell-autonomous impact of polysialic acid-producing enzyme ST8SIA2 on developmental migration and distribution of cortical interneurons. Journal of Neurochemistry, 152, pp.333–349.

[15] Singh, K.P. and Singh, M.K. (2017). In utero exposure to atypical antipsychotic drug, risperidone: effects on fetal neurotoxicity in hippocampal region and cognitive impairment in rat offspring. Progress in Neuro-Psychopharmacology & Biological Psychiatry. DOI: 10.1016/j.pnpbp.2016.12.006.

[16] Singh, K.P., Singh, M.K. and Singh, M. (2016). Effects of prenatal exposure to antipsychotic risperidone on developmental neurotoxicity, apoptotic neurodegeneration and neurobehavioral sequelae in rat offspring. International Journal of Developmental Neuroscience, 52, pp.13–23. DOI: 10.1016/j.ijdevneu.2016.05.006.

[17] Szewczyk, L.M. *et al.* (2017). ST8SIA2 promotes oligodendrocyte differentiation and the integrity of myelin and axons. Glia, 65(1), pp.34–49. DOI: 10.1002/glia.23048.

[18] Tarozzi, A. ; Angeloni, C. ; Malaguti, M. ; Morroni, F. ; Hrelia, S. ; Hrelia, P. (2013) Sulforaphane as a potential protective phytochemical against neurodegeneration diseases . Oxidative Medicine and Cellular Longevity . 2013(1): 415078 .

[19] Werneburg, S. *et al.* (2017). Polysialylation at early stages of oligodendrocyte differentiation promotes myelin repair. Journal of Neuroscience, 37(34), pp.8131–8141. DOI: 10.1523/JNEUROSCI.1147-17.2017.

[20] Yoo, S. W. ; Motari, M. G. ; Susuki, K. ; Prendergast, J. ; Mountney, A. ; Hurtado, A. ; Schnaar, R. (2015) Sialylation regulates brain structure and function . The FASED Journal .29(7): 3040 .

[21] Zhu, W. : Zhou, Y. ; Guo, L. ; Feng, S. (2024) Biological function of sialic acid and sialylation in human health and disease . Cell Death Discovery. 10(1): 415